

# Intramolecular inter-ring haptotropic rearrangement in iridium naphthalene complexes: a DFT study

Yu. F. Oprunenko\* and I. P. Gloriov

Department of Chemistry, M. V. Lomonosov Moscow State University,  
Bldg 3, 1 Leniskie Gory, 199991 Moscow, Russian Federation.

Fax: +7 (495) 939 26 77. E-mail: oprunenko@nmr.chem.msu.su, oprunenko@mail.ru

Quantum chemical simulation of the inter-ring haptotropic rearrangement (IHR) in iridium naphthalene complexes  $[\eta^4\text{-Ir}(\text{C}_{10}\text{H}_8)\text{L}_2]^+$  ( $\text{L} = \text{PH}_3, \text{PMe}_3, \text{PPh}_3$ ) involving migration of organometallic group from one of the aromatic ring to the other, was performed using the PBE density functional method with the TZV2p basis set for valence electrons and the relativistic SBK-JC pseudopotentials for the core electrons. The structures of the transition states and intermediates were studied. The IHR proceeds at the periphery of the naphthalene ligand. All transition states have reduced symmetry and hapticity compared with the initial complexes. The calculated thermodynamic parameters of the IHR are in agreement with the NMR data for the related iridium complex of ethylnaphthalene  $[\eta^4\text{-Ir}(\text{2-ethylnaphthalene})\text{L}_2]^+\text{A}^-$ ,  $\text{L} = \text{PPh}_3$ ,  $\text{A} = \text{SbF}_6$ ,  $k \approx 6 \cdot 10^{-4} \text{ s}^{-1}$ ,  $\Delta G^\ddagger_{283 \text{ K}} \approx 21 \text{ kcal mol}^{-1}$ .

**Key words:** density functional theory, PBE functional, SBK-JC relativistic pseudopotential, TZV2p basis set, quantum chemical calculations, iridium complexes, polyaromatic ligands, transition states, intermediates.

Currently,  $\pi$ -arene transition metal complexes are widely used in organic and organoelement chemistry for catalytic and synthetic purposes. These compounds are effective precursors of corresponding substituted complexes of aromatic organic compounds due to their ability to provide fine control of regioselectivity and stereochemistry of metallation (for example, lithiation) and subsequent reactions of the salts formed with electrophiles. This approach is used, in particular, for the synthesis of pharmaceuticals and other biologically active compounds.

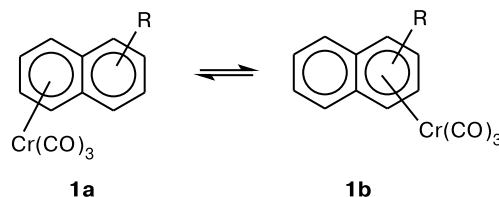
This important and broad class of compounds has been best studied for monoaromatic ligands (MAL) and to a somewhat lesser extent for polyaromatic ligands (PAL). Complexes with PAL, in which only part of the ligand atoms is bonded to transition metal, are highly labile. Various dynamic processes are observed in these organoelement derivatives.<sup>1</sup> Intramolecular inter-ring haptotropic rearrangements (IHR) are rather typical and well studied.<sup>2</sup>

Attempts to prove the existence of the degenerated IHR (for example,  $\eta^6, \eta^6$ -inter-ring rearrangements) in transition metal complexes with unsubstituted PAL were made. However, detection of this type of rearrangement by dynamic NMR spectroscopy appeared to be impossible without introducing a labelled substituent into a ring of a polyaromatic compound. It is explained by high activation barrier to the IHR in question. For instance, no dynamic phenomena were observed in  $^1\text{H}$  and  $^{13}\text{C}$  NMR spectra of  $\eta^6$ -acenaphthylene $\text{Cr}(\text{CO})_3$ ,<sup>2</sup>  $\eta^6\text{-C}_{10}\text{H}_8\text{Cr}(\text{CO})_3$ ,<sup>3</sup>

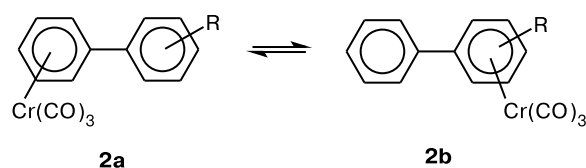
$[(\eta^6\text{-C}_{10}\text{H}_8)\text{Ir}(\text{C}_5\text{Me}_5)]^{2+}(\text{PF}_6^-)_2$  (70 °C,  $\text{CF}_3\text{COOH}$ ),<sup>4</sup>  $(\eta^6\text{-C}_{10}\text{H}_8)_2\text{Cr}$  (130 °C,  $\text{C}_6\text{D}_6$ )<sup>5</sup> samples in the NMR time scale upon heating. Only recently, these effects were detected for the 16-electron nickel complexes of naphthalene ( $\eta^2\text{-C}_{10}\text{H}_8$ ) $\text{Ni}(\text{Pr}_2\text{NCH}_2\text{CH}_2\text{NPr}_2)$ <sup>6</sup> and anthracene ( $\eta^2\text{-C}_{14}\text{H}_{10}$ ) $\text{Ni}(\text{PEt}_2)_2$  ( $\eta^2, \eta^2$ -IHR).<sup>7</sup>

Thermally induced intermolecular IHR were systematically studied: experimentally for the labelled compounds and theoretically for chromium tricarbonyl complexes of PAL by the DFT method. Such studies were mainly performed for chromium tricarbonyl complexes of naphthalene<sup>8–10</sup> (Scheme 1), biphenyl<sup>11</sup> (Scheme 2), and some other PAL (for example, biphenylene<sup>12</sup> and dibenzothiophene<sup>13</sup>). Labels were usually introduced by lithiation followed by the reaction of the lithium salt with electrophile RX. However, this is not a versatile approach. For example, it was unsuccessful for acenaphthylene and fluoranthene complexes, viz., no corresponding labelled

Scheme 1



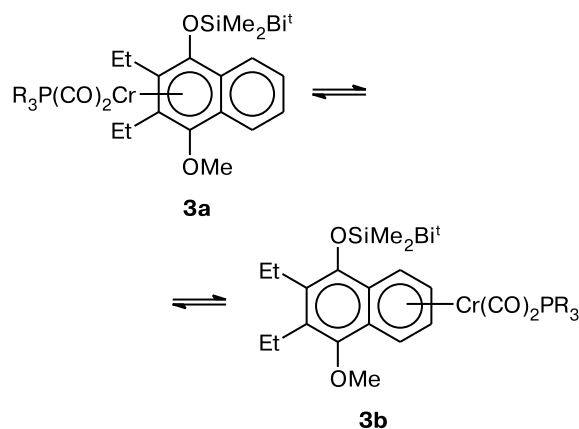
Scheme 2



complexes were synthesized and the rate constants and thermodynamic parameters determined.

Nevertheless, the activation barriers to IHR can be easily and reliably determined by conventional kinetic approaches upon introduction of the label. In the complexes dissolved in inert, non-coordinating solvents (for example, decane or hexafluorobenzene), in the course of rearrangement the  $\text{Cr}(\text{CO})_3$  group (slowly) or a phosphine-substituted group  $\text{Cr}(\text{CO})_2(\text{PR}_3)$  (more rapidly)<sup>14</sup> (Scheme 3) intramolecularly migrates along the  $\pi$ -system of the ligand between different aromatic rings at the temperatures 80–170 °C with activation barriers of 27–33 kcal mol<sup>-1</sup> ( $\eta^6, \eta^6$ -rearrangement).

Scheme 3



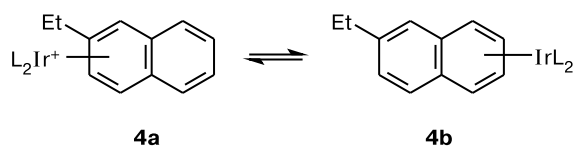
R = Ph, OPh, Me, OMe

The intermolecular character of such rearrangements is proved by the fact that they proceed in inert and non-coordinating solvent and even in melts.<sup>15</sup> This was confirmed by cross-experiments,<sup>16</sup> as well as by retention of stereochemistry<sup>17</sup> and optical activity<sup>18</sup> during the IHR. Rearrangements proceeding with such activation barriers can be studied by methods of stationary kinetics (mainly by NMR,<sup>9,13–15</sup> and in some cases by HPLC<sup>17</sup> and IR spectroscopy<sup>14</sup>).

An analysis of published data shows that almost no DFT calculations were carried out for IHR in the complexes of main-group (a rare example is the IHR of lithium cation over naphthalene radical anion or related frag-

ments, where  $\text{Li}^+$  migrates through the center of the ligand<sup>19</sup>) or transition metals (not chromium!). In the present study, the results of DFT quantum chemical calculations of IHR in the iridium complexes of naphthalene are demonstrated. The kinetic parameters of this process were experimentally studied previously for similar isomeric iridium complexes of ethylnaphthalene [ $\eta^4\text{-Ir}(\text{2-ethylnaphthalene})\text{L}_2]^+\text{A}^-$  (Scheme 4, L =  $\text{PPh}_3$ , A =  $\text{SbF}_6$ )<sup>20</sup>, but the quantum chemical simulation was performed for the unsubstituted complexes to simplify calculations. This approach is of considerable interest for the search for processes proceeding with lower activation barriers than those known for chromium complexes, *i.e.* considerably faster and under milder conditions. This is very important for catalytic and synthetic purposes.

Scheme 4



The rate constant and  $\Delta G^\ddagger_{283\text{ K}}$  value for the IHR of isomeric  $\eta^4$ -ethylnaphthalene complexes with Ir **4a**  $\rightleftharpoons$  **4b** (the process proceeds very fast and takes ~10 min to attain a 50 : 50 equilibrium at 10 °C in  $\text{CD}_2\text{Cl}_2$ ) were estimated from experimental data ( $k \approx 6 \cdot 10^{-4} \text{ s}^{-1}$ ,  $\Delta G^\ddagger_{283\text{ K}} \approx 21 \text{ kcal mol}^{-1}$ ). The activation barrier appeared to be considerably lower than that for the IHR in the corresponding chromium carbonyl complexes with naphthalene (see Schemes 1 and 3). The intermolecular character of this process was proved by cross-experiments. This means that the  $\text{IrL}_2$  fragment is more prone to haptotropy than even the  $\text{Cr}(\text{CO})_2\text{PR}_3$  fragment.

### Calculation Procedure

The molecular geometries and the transient structures were optimized by the PBE density functional method<sup>21</sup> with the TZV2p triple-zeta basis set of Gaussian functions (see Refs 22 and 23) for valence electrons and the SBK-JC relativistic pseudopotential<sup>23–25</sup> for the core electrons. The stationary points were located by analysis of the Hessians. The energies of stationary states ( $E$ ) were calculated with inclusion of the zero-point vibrational energy correction (ZPVE,  $E^0$ ). The statistical formulas of rigid rotator and harmonic oscillator were used for calculations of the free activation energy  $G$  at 298.15 K. Correspondence between the transition states (TS) and the corresponding minima on the potential energy surface (PES) was checked by constructing the intrinsic reaction coordinate (IRC). Quantum chemical calculations were performed using the PRIRODA-04 program package (see Ref. 22) on the

MVS-100k computer cluster at the Joint SuperComputer Center (JSCC) of the Russian Academy of Sciences.

## Results and Discussion

**Rearrangements in  $[(\eta^4\text{-C}_{10}\text{H}_8)\text{IrL}_2]^+$  complexes.** Four models of iridium naphthalene complexes ( $\text{L} = \text{PR}_3$ ,  $\text{R} = \text{H}$  (**I**),  $\text{Me}$  (**II**),  $\text{Pr}^i$  (**III**),  $\text{Ph}$  (**IV**) (Fig. 1) containing phosphine ligands of different nature and steric hindrances were considered. The optimized structures, selected geometric parameters, and energies of the complexes are given below. For all four models, the  $\eta^4$ -structure corresponds to the minimum on the PES, which in turn corresponds to the 16-electron nickel complexes. The naphthalene ligand loses its planarity and the  $\eta^4$ -fragment bonded to Ir bends with respect to the noncoordinated fragment of the ligand (dihedral angle  $\theta \approx 25.4\text{--}15.4^\circ$ ). This angle increases as the phosphine ligand becomes more crowded, *i.e.* the volume of the groups R surrounding the phosphine atom increases: it is maximum for structure **III** ( $\text{R} = \text{Pr}^i$ ) and minimum for **I** ( $\text{R} = \text{H}$ ). This distortion of the arene planarity is described in detail for the transition metal  $\eta^4$ -complexes with MAL and PAL.<sup>26</sup>

It is known<sup>27</sup> that the geometries of chromium tricarbonyl complexes with PAL are well described by the DFT method. The presence of the bond of the Cr atom with a particular C atom is determined according to Bader<sup>28</sup> (the bond order should be 0.15 or higher).<sup>27</sup> Probably, this value can vary to some extent depending on the transition metal. It is interesting to check the correctness of the criteria for the determination of the hapticity for the initial

iridium complexes and for the corresponding stationary states during the study of the IHR.

We analyzed the bond orders for the naphthalene iridium  $\eta^6$ -complex (Table 1). Such complexes with the  $\eta^6$ -configuration  $[(\eta^6\text{-C}_{10}\text{H}_8)\text{IrH}_2\text{PPr}_3]^+\text{BF}_4^-$  (**V**) and  $[(\eta^6\text{-C}_{10}\text{H}_8)\text{IrCpMe}_5]^{2+}(\text{PF}_6^-)_2$  (**VI**) determined on the basis of  $^1\text{H}$  and  $^{13}\text{C}$  NMR spectra and X-ray data were described earlier<sup>4,29</sup> and differ in hapticity from the  $\eta^4$ -complexes, which are the subject of the present study.

Geometry optimization of complex **V** by the DFT method led to two stable states (Fig. 2), which differ considerably in orientation of the hydride atom and have close energies. The optimized structures were also calculated for complex **VI** and its cyclopentadienyl analog  $[(\eta^6\text{-C}_{10}\text{H}_8)\text{IrCp}]^{2+}(\text{PF}_6^-)_2$  (**VII**). It should be noted that characteristic feature of the iridium  $\pi$ -complexes consists in reversible transitions  $\eta^6 \rightleftharpoons \eta^4$  associated with the slipping of iridium atom to the periphery of the six-membered ring.

Analysis of bond orders (see Table 1) indicates that complexes **V** and **Va** have the  $\eta^6$ -configuration, whereas complexes **I–IV** have the  $\eta^4$ -configuration, which is in good agreement with the NMR and X-ray data. As the additional phosphine ligand L becomes more sterically crowded, the symmetry violation of the Ir–C bonds relative to the six-membered fragment of the naphthalene ring is increasingly more pronounced.

Iridium complexes with PAL very often have the  $\eta^6$ -configuration<sup>29</sup> (it is in agreement with the 18-electron rule; the complexes are yellow or colorless), although the corresponding  $\eta^4$ -complexes are also known, being usually red. In addition, the structures of the  $\eta^4$ -complexes of other transition metals (Co, Fe, Rh, *etc.*) with naphthalene were reported.<sup>30</sup> Due to the  $\eta^4$ -configuration of complexes **I–IV**, only the  $\eta^4 \rightleftharpoons \eta^4$  inter-ring haptotropy is

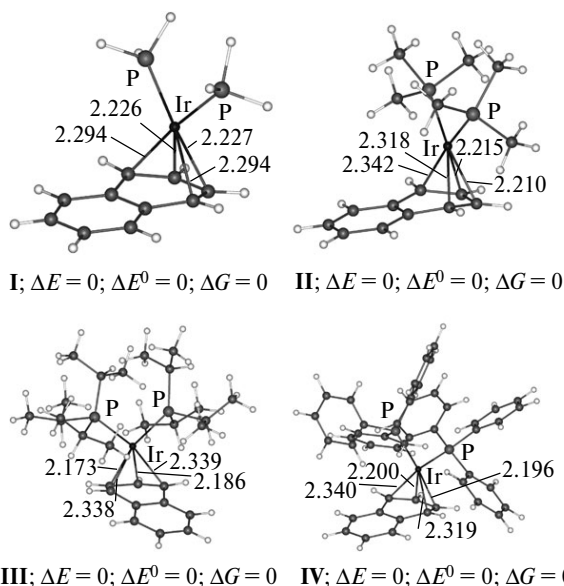


**Fig. 1.** Optimized structures of model complexes  $[(\eta^4\text{-C}_{10}\text{H}_8)\text{IrL}_2]^+$  **I–IV**. Here and in Figs 2, 3, 5, 6, 8 and 10 the bond lengths (Å) are shown;  $\Delta E$ ,  $\Delta E^0$  and  $\Delta G$  values are given in  $\text{kcal mol}^{-1}$ .

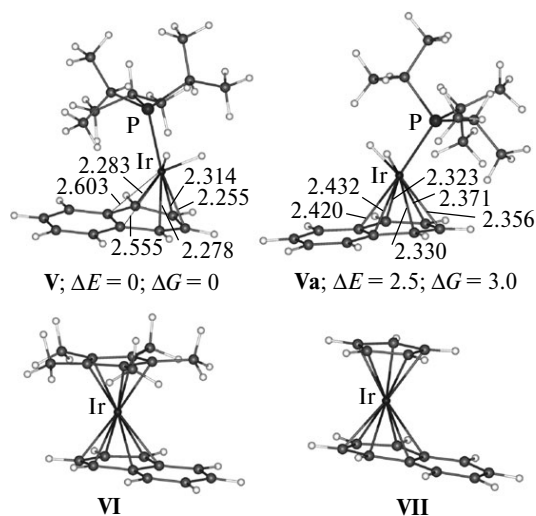


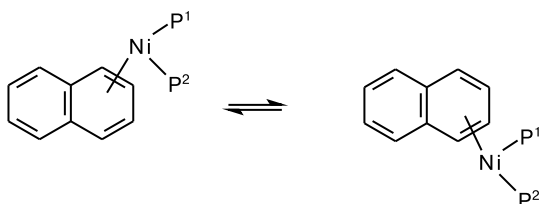
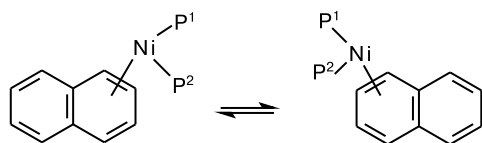
**Fig. 2.** Optimized structures of complexes  $[(\eta^6\text{-C}_{10}\text{H}_8)\text{IrH}_2\text{PPr}_3]^+$  (**V**, **Va**),  $[(\eta^6\text{-C}_{10}\text{H}_8)\text{IrCpMe}_5]^{2+}$  (**VI**), and  $[(\eta^6\text{-C}_{10}\text{H}_8)\text{IrCp}]^{2+}$  (**VII**).

**Table 1.** Ir—C bond lengths in complexes **I**–**VII**

Complex	C(1)	C(2)	C(3)	C(4)	C(4a)	C(8a)
<b>I</b> ( $\eta^4$ )	0.38	0.33	0.33	0.38	0.10	0.10
<b>II</b> ( $\eta^4$ )	0.38	0.32	0.37	0.37	0.08	0.07
<b>III</b> ( $\eta^4$ )	0.54	0.41	0.41	0.55	0.09	0.06
<b>IV</b> ( $\eta^4$ )	0.48	0.33	0.35	0.42	0.10	0.06
<b>VI</b> ( $\eta^6$ )	0.36	0.32	0.32	0.36	0.22	0.22
<b>VII</b> ( $\eta^6$ )	0.35	0.31	0.31	0.35	0.22	0.21
<b>V</b> ( $\eta^6$ )	0.34	0.28	0.28	0.32	0.12*	0.15
<b>Va</b> ( $\eta^6$ )	0.30	0.27	0.24	0.30	0.15	0.17

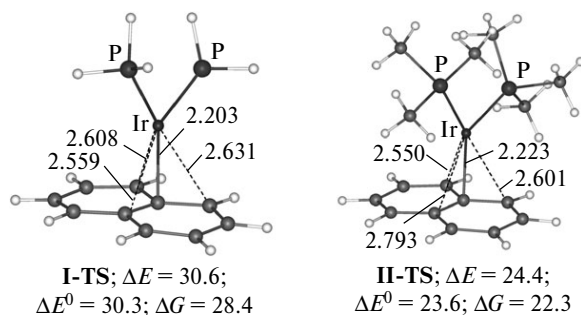
\* Small deviation from the critical value 0.15 (for Cr—C bond) to 0.12 for Ir—C bond suggests the dependence of this formal criterion on the nature of metal and tendency of Ir to the change its hapticity at  $\eta^4 \rightarrow \eta^6$ .

possible, whereas the intra-ring haptotropy similar to the  $\eta^2 \rightleftharpoons \eta^2$  haptotropy in the naphthalene nickel  $\eta^2$ -complexes is impossible.<sup>6</sup> The DFT study of the structure of these naphthalene nickel complexes, as well as the intra-ring (Scheme 5) and inter-ring rearrangements (Scheme 6) in these complexes will be published elsewhere.

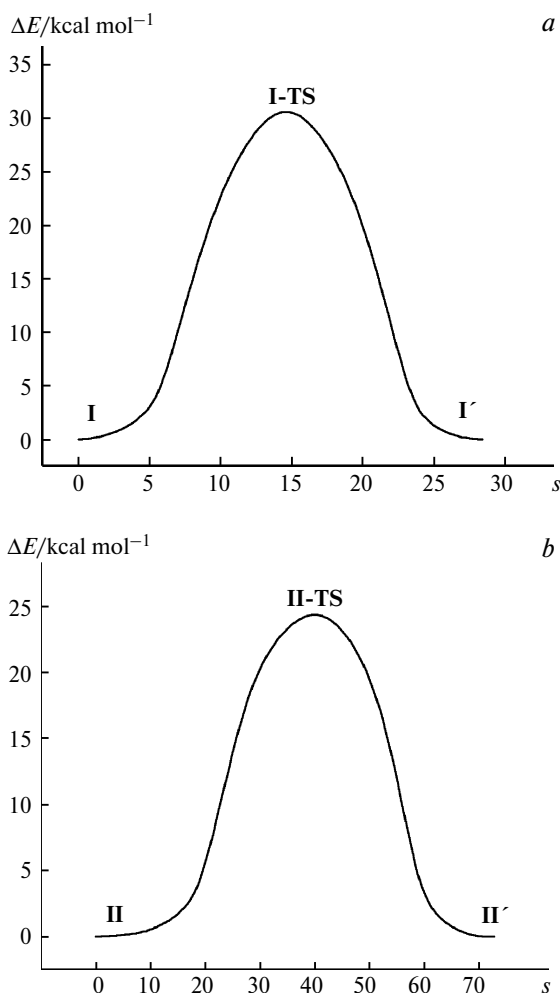
**Scheme 5****Scheme 6**

PES calculations of the  $\eta^4 \rightleftharpoons \eta^4$  inter-ring haptotropic rearrangement for complexes **I** and **II** lead to symmetrical transition states **I-TS** and **II-TS** (Figs 3 and 4). Taking into account the calculation error due to the degeneracy of the IHR, the isomeric complexes **I'** and **II'** formed upon the  $\eta^4 \rightleftharpoons \eta^4$  rearrangement have almost the same symmetry and energy as the complexes **I** and **II**.

Analysis of the bond orders (Table 2) suggests that the larger the phosphine ligands the higher the steric strain between them and the lower the hapticity of the iridium—PAL bond in the transition state. The structure of the transition state with a rather high energy ( $\sim 30$  kcal mol<sup>−1</sup>) changes from the trimethylenemethane type  $\eta^4$ -**I-TS** to an almost allyl type  $\eta^3$ -**II-TS**. Of course,

**Fig. 3.** The structures of transition states (TS) of the IHR **4a**  $\rightleftharpoons$  **4b** in complexes **I** and **II**.

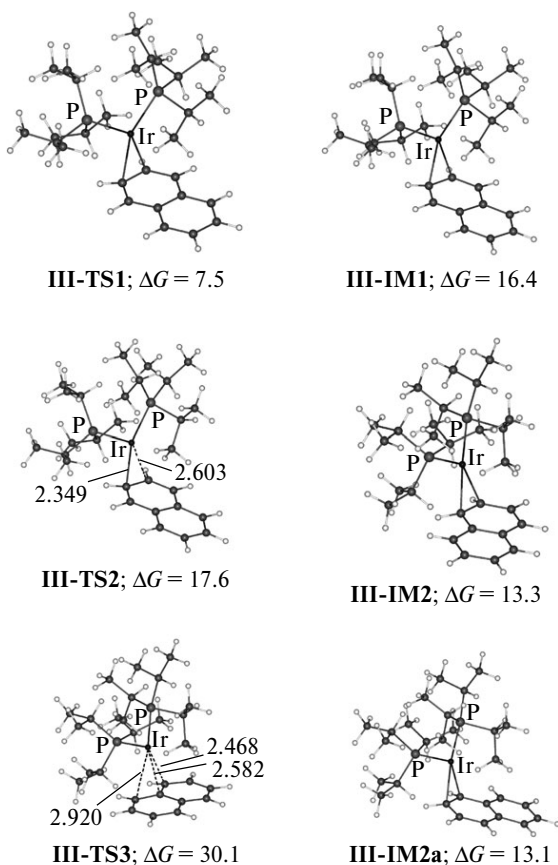
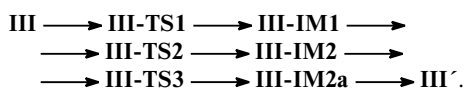
this approach is somewhat formal; however, the Ir—C(4a) bond in structure **II-TS** is weaker than in structure **I-TS** (bond orders are 0.14 and 0.22, respectively).

**Fig. 4.** Changes in  $\Delta E$  along the reaction coordinate for the IHR **I**  $\rightleftharpoons$  **I'** (a) and **II**  $\rightleftharpoons$  **II'** (b). Hereafter, the reaction coordinate  $s$  is given in the mass-weighted coordinates Bohr amu<sup>0.5</sup>, amu is the atomic mass unit, Bohr is the atomic distance unit, *i.e.* the radius of hydrogen atom.

**Table 2.** Ir—C bond orders in transition states **I-TS** and **II-TS**

State	C(8a)	C(1)	C(8)	C(4a)
<b>I-TS</b>	0.29	0.19	0.19	0.22
<b>II-TS</b>	0.28	0.23	0.17	0.14

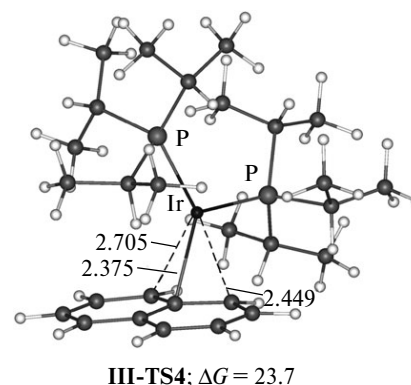
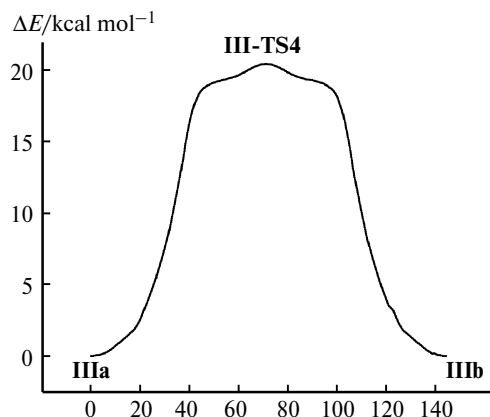
The PES of structure **III** has a more complex shape. The  $\eta^4$ -structure corresponding to the global minimum is characterized by flattening of the naphthalene ring with conservation of the symmetry plane and transformation to the  $\eta^2$ -configuration with the increase in the energy to  $\Delta G = 17.5 \text{ kcal mol}^{-1}$  (**III-TS1**) and further to the intermediate (**III-IM1**) with the same symmetry and a close energy ( $\Delta G = 16.4 \text{ kcal mol}^{-1}$ ). The intermediate **III-IM2** is formed *via* the transition state **III-TS2**. Finally, migration to the adjacent ring (Fig. 5) occurs *via* the transition state **III-TS3** ( $\Delta G = 30.1 \text{ kcal mol}^{-1}$ ). The overall transformation (taking into consideration the calculation error) is as follows:

**Fig. 5.** Structures of transition states and intermediates of the IHR in complexes **III**.

One can assume that the asymmetry of the structure, difference in the Ir—C bond lengths in **III-TS3**, and a rather high energy of this transition state ( $\Delta G = 30.1 \text{ kcal mol}^{-1}$ ) are due to rotational isomerism of sterically crowded isopropyl groups. No experimental  $\Delta G^\ddagger$  values are available for the IHR in structure **III**. Probably, this complex mechanism of the IHR is virtually unrealizable.

The experimental data available for the IHR **4a**  $\rightleftharpoons$  **4b** in the complexes studied ( $L = \text{PPh}_3$ ,  $\Delta G_{283 \text{ K}} \approx 21 \text{ kcal mol}^{-1}$ ) indicate that, probably, the rearrangement proceeds *via* another transition state with a lower energy and another rotational isomerism of isopropyl groups in the phosphine ligands. Additional calculations led to an alternative  $\eta^3$ -transition state (**III-TS4**) (Figs 6 and 7) with a lower energy, which better corresponds to the experimental data in terms of energy.

Some flattening of the PES curve to the right and to the left from the maximum corresponding to the transition state **III-TS4** is explained by the motion of the organometallic fragment along the periphery of the naphthalene ligand from one ring to the other with the change in hapticity:  $\eta^4$  (initial complex)  $\rightarrow \eta^3$  (**III-TS4**)  $\rightarrow \eta^2$  (for-

**Fig. 6.** The structure of alternative transition state of the IHR in complexes **III**.**Fig. 7.** Changes in  $\Delta E$  along the reaction coordinate for the IHR **IIIa**  $\rightleftharpoons$  **IIIb**.

mation of the metal—olefin bond in the six-membered ring)  $\rightarrow \eta^4$  (final product). In the plateau region, two opposite trends are observed around the transition state, namely, an increase in energy due to the cleavage of one of the three bonds, and a decrease in energy due to the increase in stability of the two bonds being formed ( $\eta^3 \rightarrow \eta^2$  transition).

The descent along the reaction coordinate (see Fig. 7) from this transition state leads to stable  $\eta^4$ -conformers **IIIa** and **IIIb** with a little higher energy than that of structure **III** (Fig. 8), which are then transformed to conformer **III** by the different concerted and asynchronous rotations around P—C bonds (Figs 1, 7, and 8). These rotations were not studied theoretically.

In complex **IV**, which differs from the synthesized one<sup>20</sup> only in the absence of ethyl group in one ring, the IHR proceeds in a more complicated way than in complexes **I** and **II**, but also along the periphery of the naphthalene ring. The  $\eta^2$ -transition state (**IV-TS**) is further shifted to the flattened region of intermediates placed between transition states **IV-TS** and **IV-TS'** with the lowering in energy: first, to the intermediate **IV-IM** ( $\eta^2$ ), then to the intermediate **IV-IM-a** ( $\eta^3$ ) and includes the atoms C(1), C(9), and C(8) in the coordination sphere (Figs 9 and 10).

This IHR is more complicated than in complex **III** with the isopropyl ligand. This is explained by steric hindrances of phenyl ligand overlayed by other factors leading to stabilization of intermediates. The electron-withdrawing properties of phenyl groups, which differ them from alkyl substituents in structures **I–III**, can be among these factors.

Thus, the IHR in the iridium naphthalene complexes  $[(\eta^4\text{-C}_{10}\text{H}_8)\text{IrL}_2]^+$  with different phosphine ligands **L** were studied by the DFT method. The  $\eta^4$ -structure of the initial products is in agreement with the experimental data for related ethyl-substituted complexes  $[\eta^4\text{-Ir}(\text{2-ethyl-naphthalene})\text{L}_2]^+\text{A}^-$  (**L** =  $\text{PPh}_3$ ) **4a** and **4b**. The transition states and intermediates of the IHR in these complexes, which are similar to the rearrangement **4a**  $\rightleftharpoons$  **4b** experimentally studied by NMR spectroscopy (see Scheme 4), were also studied. All these intermediates have a reduced

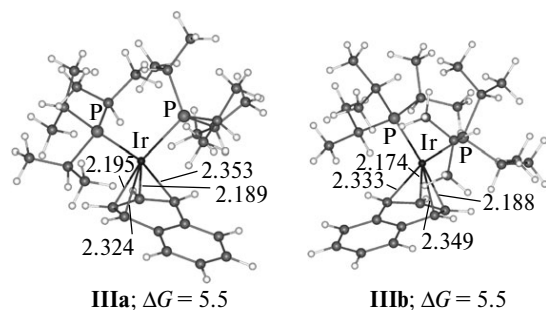


**Fig. 8.** Stable structures **IIIa** and **IIIb** with higher energy compared with complex **III**.

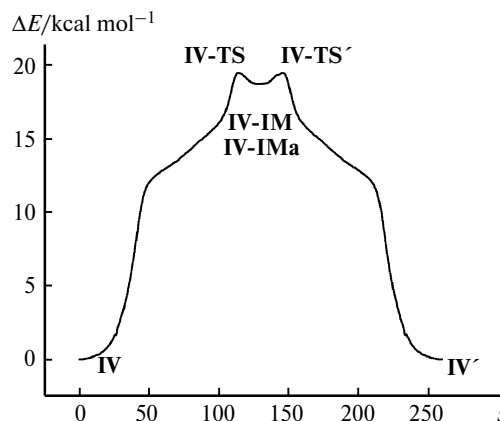


**Fig. 9.** Changes in  $\Delta E$  along the reaction coordinate for the IHR **IV**  $\rightleftharpoons$  **IV'**.

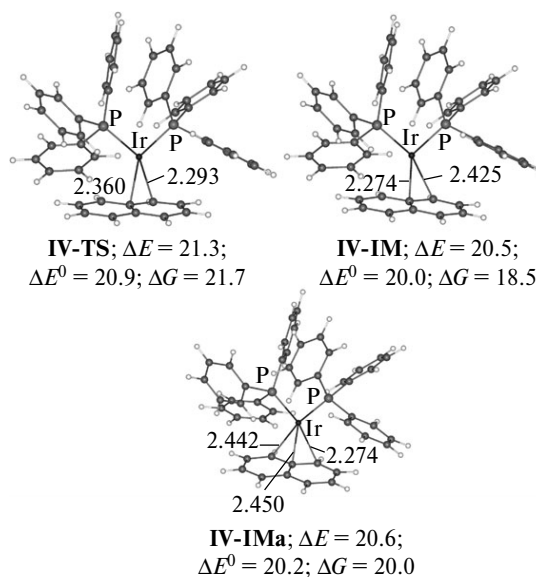


**Fig. 10.** The structures of transition states and intermediates of the IHR **4a**  $\rightleftharpoons$  **4b** in complex **IV**.

symmetry and hapticity compared with the initial complexes. The calculated thermodynamic parameters of the IHR in the unsubstituted complexes are in agreement with the experimentally obtained kinetic data.

The authors appreciate the Alexander von Humboldt Foundation (Bonn, Germany) for supplying the working station and additional computer equipment for performing DFT calculations.

## References

1. A. Berger, J. P. Djukic, Ch. Michon, *Coord. Chem. Rev.*, 2002, **225**, 215; M. F. Semmelhack, in *Comprehensive Organometallic Chemistry II*, Eds E. W. Abel, F. G. A. Stone, G. Wilkinson, 1995, **12**, Pergamon Press, Oxford, UK,

- p. 1017; P. J. Dickens, J. P. Gilday, J. T. Negri, D. A. Widowson, *Pure Appl. Chem.*, 1990, **62**, 575.
2. Yu. F. Oprunenko, *Russ. Chem. Rev.*, 2000, **69**, 683; T. A. Albright, P. Hofmann, R. Hoffmann, C. P. Lillya, P. A. Dobosh, *J. Am. Chem. Soc.*, 1983, **105**, 3396.
3. K. M. Nicholas, R. C. Kerber, E. I. Stiefel, *Inorg. Chem.*, 1971, **10**, 1519.
4. C. White, S. J. Thompson, P. M. Maitlis, *J. Chem. Soc., Dalton Trans.*, 1977, 1654.
5. E. P. Kündig, C. Perret, S. Spichiger, G. Bernardinelli, *J. Organomet. Chem.*, 1985, **286**, 183.
6. R. Benn, R. Mynott, I. Topalović, F. Scott, *Organometallics*, 1989, **8**, 2299.
7. A. Stanger, *Organometallics*, 1991, **10**, 2979.
8. K. H. Dötz, R. Dietz, *Chem. Ber.*, 1977, **110**, 1555; K. H. Dötz, H. C. Jahr, *Chem. Record*, 2004, **4**, 61; K. H. Dötz, N. Szesni, M. Nieger, K. Nattinen, *J. Organomet. Chem.*, 2003, **671**, 58.
9. Yu. F. Oprunenko, N. G. Akhmedov, S. G. Malyugina, V. I. Mstislavsky, V. A. Roznyatovsky, D. N. Laikov, Yu. A. Ustynyuk, N. A. Ustynyuk, *J. Organomet. Chem.*, 1999, **583**, 136.
10. E. P. Kündig, V. Desorby, C. Grivet, B. Rudolph, S. Spichiger, *Organometallics*, 1987, **6**, 1173; R. U. Kirss, P. M. Treichel, Jr., *J. Am. Chem. Soc.*, 1986, **108**, 853.
11. Yu. F. Oprunenko, I. A. Shaposhnikova, Yu. A. Ustynyuk, N. A. Ustynyuk, D. N. Kravtsov, *Izv. Akad. Nauk SSSR, Ser. Khim.*, 1987, 703 [*Bull. Acad. Sci. USSR, Div. Chem. Sci. (Engl. Transl.)*, 1987, **36**, 644].
12. Yu. Oprunenko, I. Gloriov, K. Lyssenko, S. Malyugina, D. Mityuk, V. Mstislavsky, H. Günther, G. von Firks, M. Ebener, *J. Organomet. Chem.*, 2002, **656**, 27.
13. M. V. Zabalov, I. P. Gloriov, Yu. F. Oprunenko, D. A. Lemenovskii, *Izv. Akad. Nauk, Ser. Khim.*, 2003, 1484 [*Russ. Chem. Bull., Int. Ed.*, 2003, **52**, 1567].
14. H. C. Jahr, M. Nieger, K. H. Dötz, *Chem. Eur. J.*, 2005, **11**, 5333.
15. Yu. Oprunenko, S. Malyugina, A. Vasil'kov, Ch. Elschenbroich, K. Harms, *J. Organomet. Chem.*, 2002, **641**, 208.
16. Yu. F. Oprunenko, S. G. Malyugina, Yu. A. Ustynyuk, N. A. Ustynyuk, D. N. Kravtsov, *J. Organomet. Chem.*, 1988, **338**, 357.
17. Yu. F. Oprunenko, S. G. Malyugina, N. A. Ustynyuk, *Izv. Akad. Nauk SSSR, Ser. Khim.*, 1988, 438 [*Bull. Acad. Sci. USSR, Div. Chem. Sci. (Engl. Transl.)*, 1988, **37**, 357].
18. Yu. Oprunenko, S. Malyugina, P. Nesterenko, D. Mityuk, O. Malyshev, *J. Organomet. Chem.*, 2000, **597**, 42.
19. H. Preuss, *Theoretical Investigation of Haptotropic Molecular Switches Controlled by Strong Laser Pulses*, Diplomarbeit, Institute of Physical Chemistry, Friedrich-Schiller-University Jena, 2009, 33; J. Li, H. Li, X. Liang, S. Zhang, T. Zhao, D. Xia, Z. Wu, *J. Phys. Chem. A*, 2009, **113**, 791.
20. R. H. Crabtree, C. P. Parnell, *Organometallics*, 1984, **3**, 1727.
21. J. P. Perdew, K. Burke, M. Ernzerhof, *Phys. Rev. Lett.*, 1996, **77**, 3865.
22. D. N. Laikov, *Chem. Phys. Lett.*, 1997, **281**, 151; D. N. Laikov, Yu. A. Ustynyuk, *Izv. Akad. Nauk, Ser. Khim.*, 2005, 804 [*Russ. Chem. Bull., Int. Ed.*, 2005, **54**, 820].
23. W. J. Stevens, H. Basch, M. Krauss, *J. Chem. Phys.*, 1984, **81**, 6026.
24. W. J. Stevens, M. Krauss, H. Basch, P. G. Jasien, *Can. J. Chem.*, 1992, **70**, 612.
25. T. R. Cundari, W. J. Stevens, *J. Chem. Phys.*, 1993, **98**, 5555.
26. M. R. Churchill, R. Mason, *Proc. R. Soc. London, Ser. A*, 1966, **292**, 61; G. Huttner, S. Lange, E. O. Fischer, *Angew. Chem.*, 1971, **83**, 579; *Angew. Chem., Int. Ed. Engl.*, 1971, **10**, 556; A. Band, M. Bottril, M. Green, A. J. Welch, *J. Chem. Soc., Dalton Trans.*, 1977, 2372; H. Schaufele, D. Hu, H. Pritzkow, U. Zenneck, *Organometallics*, 1989, **8**, 396; W. J. Bowyer, J. W. Merkert, W. E. Geiger, A. L. Rheingold, *Organometallics*, 1989, **8**, 191.
27. Yu. F. Oprunenko, I. P. Gloriov, *J. Organomet. Chem.*, 2009, **694**, 1195.
28. R. F. W. Bader, *Atoms in Molecules: A Quantum Theory*, Oxford University Press, Oxford (UK), 1990.
29. F. Torres, E. Sola, M. Martín, C. Ochs, G. Picazo, J. A. López, F. J. Lahoz, L. A. Oro, *Organometallics*, 2001, **20**, 2716.
30. J. O. Albright, S. Datta, B. Dezubers, J. K. Kouba, D. S. Maryneck, S. S. Wreford, B. M. Foxman, *J. Am. Chem. Soc.*, 1979, **101**, 611; J. W. Hull, W. L. Gladfelter, *Organometallics*, 1984, **3**, 605; J. W. Kang, R. F. Childs, P. M. Maitlis, *J. Am. Chem. Soc.*, 1970, **92**, 720.

Received March 22, 2010;  
in revised form June 10, 2010